

Strain distributions in lattice-mismatched semiconductor core-shell nanowires

Niels S ndergaard¹, Yuhui He², Chun Fan³, Ruqi Han², Thomas Guhr^{1,4}, and H. Q. Xu^{5*}

¹*Division of Mathematical Physics, LTH, Lund University, S-22100 Lund, Sweden*

²*Institute of Microelectronics, Peking University, Beijing 100871, China*

³*Computer Center of Peking University, Beijing 100871, China*

⁴*Fachbereich Physik, Universit t Duisburg-Essen, 47048 Duisburg, Germany and*

⁵*Division of Solid State Physics, Lund University, Box 118, S-22100 Lund, Sweden*

Abstract

The authors study the elastic deformation field in lattice-mismatched core-shell nanowires with single and multiple shells. We consider infinite wires with a hexagonal cross section under the assumption of translational symmetry. The strain distributions are found by minimizing the elastic energy per unit cell using the finite element method. We find that the trace of the strain is discontinuous with a simple, almost piecewise variation between core and shell, whereas the individual components of the strain can exhibit complex variations.

I. INTRODUCTION

Nanowires have many applications. For example, nanowire-based biological sensors¹, chemical detectors², solar cells³⁻⁶, LEDs⁷, field emitters⁸, transistors⁹, and electronic logic gates¹⁰ have been demonstrated. To further tailor the properties of nanowires, experimentalists have grown nanowire axial heterostructures, such as nanowire quantum dots¹¹, and radial heterostructures, such as core-shell¹²⁻¹⁴ and multi-shell¹⁵ nanowires. In particular, a difference in lattice constant in heterostructures leads to intrinsic strain, which for nanowires can be incorporated into the material much easier than for thin films due to the more effective strain relaxation at free surfaces¹⁶. This gives the opportunity for strain-engineering of the electronic and optical properties^{17,18}. The intrinsic elastic deformation field in heterostructured nanowires is, therefore, an important and necessary input for further investigations of the properties of these heterostructured nanowires.

In this article, we discuss and calculate the strain field in lattice-mismatched core-shell and multi-shell nanowires. We find rich behaviour of the individual strain components, whereas their combination, the trace of the strain tensor (the volumetric strain), shows much less variation. Our article is organized as follows. The model and theory is introduced in Sec. II. The results and discussion are presented in Sec. III. Finally Sec. IV contains the summary and conclusions.

II. THEORY AND METHOD

In this work, we calculate the elastic deformation field in lattice-mismatched core-shell and double-shell nanowires (see Fig. 1 for schematics). As an approximation, we take the nanowires as infinite with translational symmetry along the growth direction. We argue below

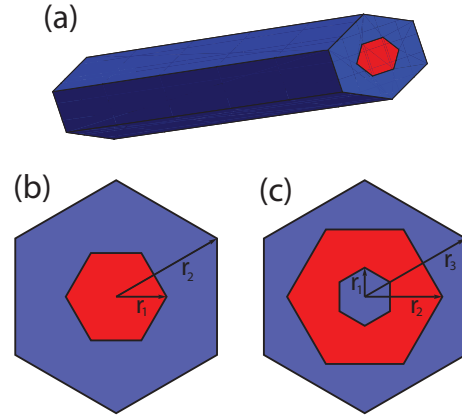


FIG. 1: (a) Schematic of a nanowire with a single shell around a core. (b) Cross section of the core-shell nanowire with core radius r_1 and shell radius r_2 . (c) Cross section of a double-shell nanowire with core radius r_1 and shell radii r_2 and r_3 .

(based on Saint-Venant's principle¹⁹), that our description of the infinite wires is also relevant for long finite wires. For simplicity, we neglect *exterior* forces acting on surface or bulk parts of the wires, i.e., we consider *free* nanowires. We restrict ourselves to nanowires with cubic lattice structure, but remark that generalizations to W rztite or other structures are straightforward. Furthermore, we consider only wires grown in the [111]-direction in this work. For convenience, we define a primed coordinate system with respect to the growth direction, having basis vectors,

$$\hat{\mathbf{x}}' = \frac{1}{\sqrt{2}} \begin{pmatrix} 1 \\ -1 \\ 0 \end{pmatrix}, \quad \hat{\mathbf{y}}' = \frac{1}{\sqrt{6}} \begin{pmatrix} 1 \\ 1 \\ -2 \end{pmatrix}, \quad \hat{\mathbf{z}}' = \frac{1}{\sqrt{3}} \begin{pmatrix} 1 \\ 1 \\ 1 \end{pmatrix}. \quad (1)$$

Consider, for example, a core-shell nanowire with undeformed core and shell axial lengths of L_c and L_s and lattice constants of $a^{(c)}$ and $a^{(s)}$. To allow for pseudomorphic matching, we shall assume that both core and shell have the same number N of unit cells in the axial

*electronic mail: hongqi.xu@ftf.lth.se

direction and, thus, L_c must necessarily differ from L_s . We can write

$$\frac{L_c}{a^{(c)}} = \frac{L_s}{a^{(s)}} = C \cdot N, \quad (2)$$

where C is some constant of proportionality. In the zincblende structure case for the [111]-direction, C would be $\sqrt{3}$.

To match the lattice of the shell to the core we introduce the pseudomorphic initial strain field $\epsilon^{(0)}$ in the shell. This choice of the pseudomorphic strain field initially scales all shell lattice vectors to have the same length as in the core²⁰,

$$(1 + \epsilon^{(0)})a^{(s)} \equiv a^{(c)}, \quad (3)$$

and

$$\epsilon^{(0)} = \epsilon^{(0)} \cdot \mathbf{1}. \quad (4)$$

The total strain tensor is given by²¹

$$\epsilon = \frac{1}{2} (\nabla \otimes \mathbf{u} + (\nabla \otimes \mathbf{u})^t) + \epsilon^{(0)}. \quad (5)$$

For long beams, an often used approximation is that of *plane strain*^{19,22}. In this approximation, the only non-zero strains are ϵ'_{xx} , ϵ'_{yy} and ϵ'_{xy} , whereas $\epsilon'_{zx} = \epsilon'_{zy} = 0$ (planar sections remain flat) and $\epsilon'_{zz} = 0$ (no axial extension). The theory has been generalized to stretched beams by assuming that the axial extension ϵ'_{zz} is non-vanishing but can be taken as a given fixed parameter²³. For the core-shell and the double-shell nanowires we consider in this work, ϵ'_{zz} is not known *a priori*, but we expect it to be present due to the lattice mismatch. Therefore, we introduce an ϵ'_{zz} for each sub-domain of a nanowire and consider these strains as variables. In the simple case of a core-shell structure with two sub-domains (the core and the shell), the matching effectively reduces the two axial strains $\epsilon'_{zz}^{(c)}$ and $\epsilon'_{zz}^{(s)}$ to a single variable a ,

$$e_3^{(i)} \equiv \epsilon'_{zz}^{(i)} = \frac{a}{a^{(i)}} - 1, \quad \text{with } i = s, c. \quad (6)$$

In the material coordinate system, the potential elastic energy is

$$U = \int w dV \equiv \frac{1}{2} \int \mathbf{e} \cdot \mathbf{C} \cdot \mathbf{e} dV, \quad (7)$$

where w is the strain energy density, $\mathbf{C} = [C_{ij}]$ is the matrix of elastic constants and $\mathbf{e} = [e_i]$ are engineering strains²⁴. In the nanowires with cubic lattice structure, the elastic constants are given by three independent constants taken by convention as C_{11} , C_{12} and C_{44} .

From now on, we shall only work in the transformed coordinate system and drop all primes in the notation. In this coordinate system, we find, after some calculation, the energy density in Eq. (7) as

$$w = \frac{1}{2} (D_1(e_1^2 + e_2^2) + D_2e_3^2 + D_3e_1e_2 + D_4(e_1 + e_2)e_3 + D_5e_6^2), \quad (8)$$

with the constants

$$\begin{aligned} D_1 &= \frac{1}{2} (C_{11} + C_{12} + 2C_{44}), \\ D_2 &= \frac{1}{3} (C_{11} + 2C_{12} + 4C_{44}), \\ D_3 &= \frac{1}{3} (C_{11} + 5C_{12} - 2C_{44}), \\ D_4 &= \frac{2}{3} (C_{11} + 2C_{12} - 2C_{44}), \\ D_5 &= \frac{1}{6} (C_{11} - C_{12} + 4C_{44}). \end{aligned} \quad (9)$$

The potential energy allows us to find the deformation field by a variational principle. Minimizing the energy in Eq. (7) leads to the equations for a collection of springs with generalized loads derived from the matching strain²².

An important ingredient of this work is the introduction of the axial extension as a variable. We shall therefore briefly discuss the variational procedure for that degree of freedom. Now consider a core-shell wire. Axial variations obey

$$\delta \epsilon_{zz}^{(i)} = \frac{\delta a}{a^{(i)}}, \quad \text{with } i = s, c. \quad (10)$$

Varying the energy per unit cell with respect to the axial parameter a gives

$$\begin{aligned} 0 &= \frac{1}{N} \frac{\delta U}{\delta a} \\ &= \frac{1}{N} \left(\frac{1}{a^{(c)}} \int_c \sigma_{zz} dV + \frac{1}{a^{(s)}} \int_s \sigma_{zz} dV \right) \\ &= \frac{1}{N} \left(\frac{L_c}{a^{(c)}} \int_c \sigma_{zz} dS + \frac{L_s}{a^{(s)}} \int_s \sigma_{zz} dS \right) \\ &\propto \int_c \sigma_{zz} dS + \int_s \sigma_{zz} dS \\ &= \int_{c+s} dF_z = F_z, \end{aligned} \quad (11)$$

where we recognize that the axial stress is given in the form of

$$\sigma_{zz} \equiv \frac{\partial w}{\partial e_3} = D_2 e_3 + \frac{D_4}{2} (e_1 + e_2). \quad (12)$$

Here we have used the assumption of translational invariance in the z -direction. Also, we note that in the second equality of Eq. (11), the integration in the axial direction has been taken over the undeformed domains of the shell and core. In Eq. (11), $\sigma_{zz} dS$ is the vertical force dF_z on an area element dS . Hence, physically, Eq. (11) implies the vanishing of the total force in the axial direction. In the multi-shell nanowire case, the condition Eq. (11) generalizes to

$$0 = \sum_i \int_{\Omega_i} \sigma_{zz} dS. \quad (13)$$

We remark that Eq. (13) should also apply to finite wires. Thus, using the principle of Saint-Venant¹⁹, we expect our results to describe well the strain field in the middle sections of finite, but long, free wires. If a net total force and moment on the terminating ends are present, the corresponding condition Eq. (13) should be changed accordingly.

In the numerics, we have used the linear finite element method²² to minimize Eq. (7) with Eq. (11) imposed for a free two-dimensional boundary. The planar degrees of freedom are seen to couple to the axial degree of freedom via, e.g., Eq. (11).

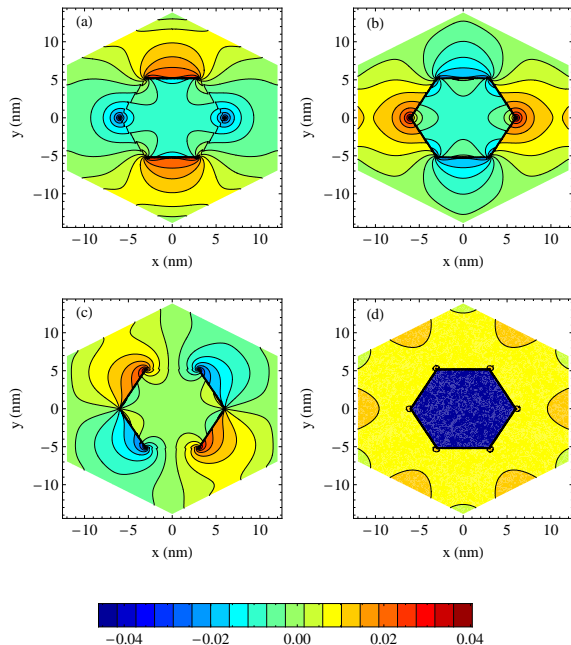


FIG. 2: Elastic strain distributions in a single-shell nanowire. The core with radius $r_1 = 6.0$ nm is made of GaAs and the shell with radius $r_2 = 13.9$ nm is made of GaP. The plots show cross-section distributions of (a) ϵ_{xx} , (b) ϵ_{yy} , (c) ϵ_{xy} , and (d) $\text{tr } \epsilon$.

III. NUMERICAL RESULTS

First, we consider a nanowire with a single GaP shell and a GaAs core with the same geometry as in the experiment reported in Ref. 14. We choose radii of the inner core and shell to be $r_1 = 6.0$ nm and $r_2 = 13.9$ nm (see Fig. 1 for the definitions of r_1 and r_2). We depict the strain components ϵ_{xx} (a), ϵ_{yy} (b), and ϵ_{xy} (c), and the trace $\text{tr } \epsilon$ (d) in Fig. 2 (the strain component ϵ_{zz} is omitted). Figure 2 (a) shows that near a horizontal interface the exterior material is expanded. Figure 2 (b) shows that the exterior material is largely expanded in the regions near the left and right corners of the core

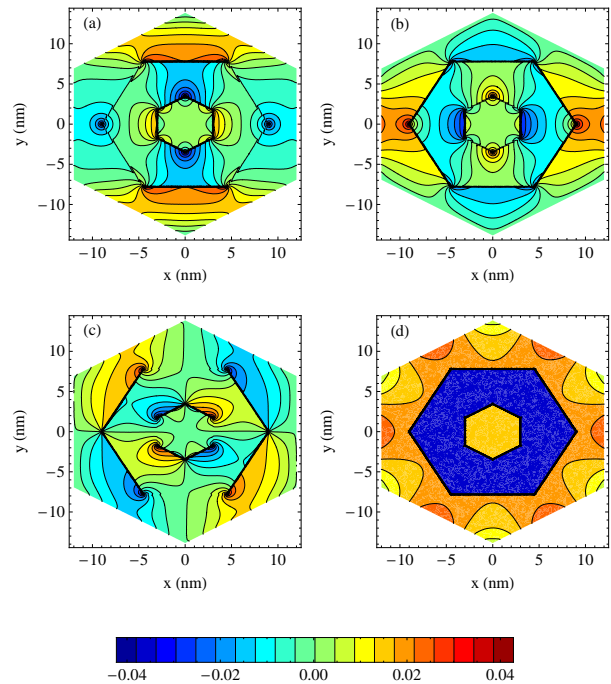


FIG. 3: Elastic strain distributions in a double-shell nanowire. The core with radius $r_1 = 3.5$ nm is made from GaP, the inner shell with radius $r_2 = 9.2$ nm is made from GaAs, and the outer shell with radius $r_3 = 13.9$ nm is made from GaP. The plots show cross-section distributions of (a) ϵ_{xx} , (b) ϵ_{yy} , (c) ϵ_{xy} , and (d) $\text{tr } \epsilon$.

of the hexagonal shape. These behaviours are consistent with the difference in the lattice constants. Figures 2 (a) and (b) also show that the two strain distribution patterns are symmetric with respect to the x- and the y-axis. The strain component ϵ_{zz} , which is not shown here, exhibits a simple step-like distribution profile with a constant axial contraction in the core and an axial elongation in the shell, again consistent with the lattice mismatch. The shear strain ϵ_{xy} in Fig. 2 (c), which is important in, e.g., the piezo-electric interaction, displays a pattern as complicated as the other individual strain components, ϵ_{xx} and ϵ_{yy} . The distribution pattern of ϵ_{xy} is, however, antisymmetric with respect to the x-axis and the y-axis. The measure of volume deformation, the dilatation $\delta V/V = \text{tr } \epsilon$, is depicted in Fig. 2 (d). In general, the shell is expanded particularly near the boundary in the middle of the edges. This expansion extends typically all the way into the corners of the core. The interior of the core is seen in Fig. 2 (d) to be contracted almost constantly.

We now turn to the case of multi-shell nanowires. For simplicity, we vary the setup only slightly by considering a core with *two* shells, a double-shell nanowire. We choose the material of the inner shell to be made of GaAs and the core and outer shell are chosen to be made from

GaP. Here, in consistence with the previous geometry, we choose the outer shell to be parallel with the inner core, see Fig. 1 (c). Still, we mention that fully parallel multi-shells are also of interest¹⁵. The radii of the core, inner shell, and outer shell are taken to be $r_1 = 3.5$ nm, $r_2 = 9.2$ nm and $r_3 = 13.9$ nm. Figure 3 shows the strain components ϵ_{xx} (a), ϵ_{yy} (b), and ϵ_{xy} (c), and the trace $\text{tr} \epsilon$ (d) of the double-shell nanowire. (Here, again, the strain component ϵ_{zz} is omitted, since it shows a simple step-like distribution profile.) Since the lattice constant of the inner shell is larger than its surroundings, the inner shell is compressed whereas the core and outer shell regions are expanded (see plots for the strain components ϵ_{xx} , ϵ_{yy} , and the trace $\text{tr} \epsilon$ in Fig. 3). In particular, the exterior shell near the interface undergoes considerable stretching as in the single-shell case. Also the same as in the single-shell nanowire case, the strain patterns of the components ϵ_{xx} and ϵ_{yy} are symmetric with respect to the x- and the y-axis, and the pattern of the trace $\text{tr} \epsilon$ is hexagonal symmetric. Furthermore, the inner shell plays almost the same role for the tensile strains as the inner core in the single-shell case. The shear strain ϵ_{xy} in Fig. 3 (c) shows similar symmetric characteristics as in the single-shell nanowire, i.e., the distribution pattern of the shear strain ϵ_{xy} is antisymmetric with respect to the x- and the y-axis, and exhibits similar peak-valley configurations in both inner shell and outer shell as in the shell region of the single-shell nanowire.

IV. SUMMARY AND CONCLUSIONS

We present a theoretical study of the strain field in lattice-mismatched core-shell nanowires with single and double shells. We derive a functional for the elastic energy in a nanowire. The deformation field is found by minimization of the energy functional using the finite element method. For the single-shell wire, the core is made of GaAs and the shell of GaP. For the double-shell wire, the inner shell is made of GaAs, whereas the core and outer shell are made of GaP. We find a large volumetric strain in various regions of a wire. A large compression appears in the core region of a single-shell nanowire or in the inner shell region of a double-shell nanowire. The large volumetric strain will influence carriers via the deformation potential. Our numerics also shows great variations in the individual components of the strain compared to the volumetric strain. This could be of particular importance for the hole confinement in p-type wires. We note that the theory presented in this work can be extended to incorporate the finite strain components ϵ_{xz} and ϵ_{yz} which have been neglected in the plane strain approximation. We leave the details of such a more general theory to forthcoming publications.

The authors thank F. Boxberg for valuable discussions.

-
- ¹ G. Zheng, F. Patolsky, Y. Cui, W.U. Wang, and C.M. Lieber, *Nature Biotechnology* **23**, 1294 (2005).
 - ² Q. Wan, Q.H. Li, Y. J. Chen, T.H. Wang, X.L. He, J.P. Li, C.L. Lin, *Appl. Phys. Lett.* **84**, 3654 (2004).
 - ³ M. Law, L.E. Greene, J.C. Johnson, R. Saykally, and P. Yang, *Nature Materials* **4**, 455 (2005).
 - ⁴ Y. Zhang, L.-W. Wang, and A. Mascarenhas, *Nano Letters* **7**, 1264 (2007).
 - ⁵ J. Schrier, D. O. Demchenko, L.-W. Wang and A. P. Alivisatos, *Nano Letters* **7**, 2377 (2007).
 - ⁶ K. Wang, J. Chen, W. Zhou, Y. Zhang, Y. Yan, J. Pern, and A. Mascarenhas, *Adv. Materials* **20**, 3248 (2008).
 - ⁷ Y. Huang, X. Duan, and C. M. Lieber, *Small* **1**, 142 (2005).
 - ⁸ J. Chen, S.Z. Deng, N.S. Xu, S. Wang, X. Wen, S. Yang, C. Yang, J. Wang, and W. Ge, *Appl. Phys. Lett.* **80**, 3620 (2002).
 - ⁹ J. Goldberger, A. Hochbaum, R. Fan, and P.D. Yang, *Nanoletters* **6**, 973 (2006).
 - ¹⁰ Y. Huang, X. Duan, Y. Cui, L.J. Lauhon, K.-H. Kim, and C.M. Lieber, *Science* **294**, 1313 (2001).
 - ¹¹ M.T. Björk, B.J. Ohlsson, T. Sass, A.I. Persson, C. Thelander, M.H. Magnusson, K. Deppert, L.R. Wallenberg, and L. Samuelson, *Appl. Phys. Lett.* **80**, 1058 (2002).
 - ¹² L.J. Lauhon, M.S. Gudiksen, D. Wang, and C.M. Lieber, *Nature* **420**, 57 (2002).
 - ¹³ W. Lu, J. Xiang, B.P. Timko, Y. Wu, C.M. Lieber, *PNAS* **102**, 10046 (2005).
 - ¹⁴ N. Sköld, L.S. Karlsson, M.W. Larsson, M.-E. Pistol, W. Seifert, J. Trädgård, and L. Samuelson, *Nano Letters* **5**, 1943 (2005).
 - ¹⁵ P. Mohan, J. Mothisa and T. Fukui, *Appl. Phys. Lett.* **88**, 133105 (2006).
 - ¹⁶ F. Glas, *Phys. Rev. B* **74**, 121302(R) (2006).
 - ¹⁷ M. Grundman, O. Stier and D. Bimberg, *Phys. Rev. B* **50**, 14187 (1994).
 - ¹⁸ M. Grundman, O. Stier and D. Bimberg, *Phys. Rev. B* **52**, 11969 (1995).
 - ¹⁹ A.N. Cleland *Foundations of nanomechanics* (Springer, Berlin) 2003.
 - ²⁰ L.D. Caro and L. Tapfer, *Phys. Rev. B* **48**, 2298 (1993).
 - ²¹ M. Povolotskyi and A. Di Carlo, *J. Appl. Phys.* **100**, 063514 (2006).
 - ²² O.C. Zienkiewicz and R.L. Taylor *The finite element method* (McGraw-Hill, Maidenhead) 1994.
 - ²³ A.E.H. Love *A treatise on the mathematical theory of elasticity* (New York: Dover) 1994.
 - ²⁴ N.W. Ashcroft and N.D. Mermin *Solid State Physics* (Saunders College, Philadelphia) 1976.